



HAL
open science

Local Structures of Oxygen-Deficient Perovskite $\text{Sr}_2\text{ScGaO}_5$ Polymorphs Explored by Total Neutron Scattering and EXAFS Spectroscopy

Serena Corallini, Monica Ceretti, Giovanni Agostini, Michela Brunelli, Giuditta Perversi, Gabriel J. Cuello, Anna Marsicano, Werner Paulus

► **To cite this version:**

Serena Corallini, Monica Ceretti, Giovanni Agostini, Michela Brunelli, Giuditta Perversi, et al.. Local Structures of Oxygen-Deficient Perovskite $\text{Sr}_2\text{ScGaO}_5$ Polymorphs Explored by Total Neutron Scattering and EXAFS Spectroscopy. *Inorganic Chemistry*, 2020, 59, pp.9434-9442. 10.1021/acs.inorgchem.0c01368 . hal-02883380v2

HAL Id: hal-02883380

<https://hal.science/hal-02883380v2>

Submitted on 27 Jan 2023

HAL is a multi-disciplinary open access archive for the deposit and dissemination of scientific research documents, whether they are published or not. The documents may come from teaching and research institutions in France or abroad, or from public or private research centers.

L'archive ouverte pluridisciplinaire **HAL**, est destinée au dépôt et à la diffusion de documents scientifiques de niveau recherche, publiés ou non, émanant des établissements d'enseignement et de recherche français ou étrangers, des laboratoires publics ou privés.

The local structure of oxygen deficient perovskite $\text{Sr}_2\text{ScGaO}_5$ polymorphs explored by total neutron scattering and EXAFS spectroscopy

Monica Ceretti^{a}, Giovanni Agostini^b, Michela Brunelli^c, Serena Corallini^a, Giuditta Perversi^{a†}, Gabriel Cuello^d, Anna Marsicano^a, Werner Paulus^a*

a. ICGM, Univ. Montpellier, CNRS, ENSCM, Montpellier, France

b. CELLS – ALBA Synchrotron Radiation Facility, Carrer de la Llum 2-26, 08290
Cerdanyola del Vallès, Barcelona, Spain.

c. Netherlands Organisation for Scientific Research (NWO), DUBBLE@ESRF BP CS40220,
38043 Grenoble, France

d. Institut Laue Langevin, Grenoble, France

KEYWORDS. Oxygen deficient perovskite, brownmillerite, oxygen electrolyte, pair distribution function, total neutron scattering, EXAFS.

ABSTRACT. Depending on the synthesis route, the oxygen ion electrolyte $\text{Sr}_2\text{ScGaO}_5$ shows two polymorphs, the brownmillerite and the cubic perovskite framework. In order to better explore oxygen diffusion pathways and mechanisms, we report here on a multi-technical approach to characterize local structural changes for $\text{Sr}_2\text{ScGaO}_5$ polymorphs as a function of

temperature, using neutron pair distribution function (PDF) analysis together with the extended X-ray absorption fine structure (EXAFS) analysis. While for the brownmillerite type structure PDF and Rietveld refinements yield identical structural descriptions, considerable differences are found for the cubic oxygen deficient polymorph. On a local scale a brownmillerite type vacancy structure could be evidenced for the cubic phase, suggesting a complex short-range ordering and respective microstructure. Both PDF and EXAFS data confirm an octahedral and tetrahedral coordination for Sc and Ga respectively, at a local scale for both polymorphs. Related changes in the bond distances and oxygen vacancy ordering are discussed.

1. Introduction

Oxygen deficient perovskite oxides have been extensively investigated in the last decades because of their rich chemistry, structural complexity, interesting properties and applications, such as ionic conductors, oxygen sensor or electrocatalysts.¹⁻⁸ From the basic perovskite framework, various structure types can be derived, which show different oxygen vacancy ordering or structural distortions. The release of one-sixth of all the oxygen atoms along the [110] direction of the cubic perovskite yields the brownmillerite type structure, with the general formula $A_2BB'O_5$. Its structure consists of alternating octahedral (O) and tetrahedral (T) layers, while the formation of empty 1D oxygen vacancy channels along the [100] direction (see Figure 1) implies an orthorhombic symmetry. The related cell parameters with respect to the parent perovskite parent structure are: $a_{brown} \cong a_{perov}\sqrt{2}$, $b_{brown} \cong 4a_{perov}$, and $c_{brown} \cong a_{perov}\sqrt{2}$. The attribution of the space group remains often ambiguous due to subtle structural changes and it becomes difficult to differentiate between different types of tetrahedral chain ordering and respective space group symmetries $Pnma$, $Imma$ and $I2mb$. Associated structural

differences are however important when it comes to interpret their potential for oxygen ion conductivity, since *Pnma* and *I2mb* result in ordered $(\text{BO}_4)_\infty$ -tetrahedral chains, while *Imma* yields an average and disordered orientation, which can be static or dynamic. More complex ordering of the tetrahedral chain ordering has been reported essentially related to charge ordering phenomena e.g. in manganites, comprising different twist orientations of the tetrahedral chains inside and between tetrahedral layers.^{9, 10}

Some oxides with brownmillerite type structure, such as SrFeO_{3-x} or SrCoO_{3-x} , show oxygen mobility down to room temperature,¹¹⁻¹³ making them an attractive class of compounds for many technologically important applications in the field of solid state electrolytes, and more specifically for membranes in solid oxide fuel cells (SOFC).

We have recently reported on oxygen diffusion mechanisms in a new oxygen deficient perovskite, $\text{Sr}_2\text{ScGaO}_5$, containing exclusively open or closed shell B-cations.¹⁴⁻¹⁷ Due to the fixed valence of Sc and Ga the phase is stoichiometric with respect to oxygen and adopts the brownmillerite structure type (space group *I2mb*) when synthesized with standard solid-state reaction conditions (1200°C). This structure shows an ordered arrangement of ScO_6 octahedral layers alternating with GaO_4 tetrahedral layers, the latter containing 1D- $(\text{GaO}_4)_\infty$ -zigzag chains. Combining neutron powder and synchrotron diffraction, a second order phase transition from *I2mb* to *Imma* has been evidenced at 300 °C, implying an order/disorder transition of the 1D $(\text{GaO}_4)_\infty$ tetrahedral chains.¹⁴

Brownmillerite-type $\text{Sr}_2\text{ScGaO}_5$ transforms above 1400°C into a cubic oxygen deficient perovskite, which retains the cubic symmetry down to room temperature even when applying slow furnace cooling.¹⁵ The existence of this cubic $\text{Sr}_2\text{ScGaO}_5$ phase, with improved oxygen ions conduction, probably related to the 3D perovskite framework and to the related diffusion pathways¹⁶, should be considered a key point for the study of stoichiometric $\text{ABO}_{2.5}$ oxygen electrolytes.

Structural investigations by powder and single crystal diffraction showed large anisotropic disk shaped oxygen displacement factors in this new cubic oxygen deficient $\text{Sr}_2\text{ScGaO}_5$ perovskite.¹⁶ Together with the fact that Raman studies indicated deviations from the average cubic symmetry, suggesting the formation of ScO_6 and GaO_4 polyhedra, it is evident that oxygen vacancy ordering on a local scale is present.

In this regard, some recent studies have shown that there are oxygen deficient perovskites with a large degree of short range order so that the local structure can be very different from the average structure.^{10, 18-22}

Local scale structural information is however important to understand the underlying activation energy and diffusion pathways of the oxygen atoms in these systems. To further investigate the local structure, a neutron pair distribution function (PDF) analysis together with the extended X-ray absorption fine structure (EXAFS) analysis were carried out on both SSGO polymorphs. We were in particular interested to carry out complementary EXAFS studies at the Ga-edge allowing to discriminate selectively the coordination of the Ga atoms and respective displacements of the coordinating oxygen atoms. Both methods are highly complementary since EXAFS is selectively probing the Ga environment on a very local scale, generally the first few coordination shells, while neutron PDF explore different length scales with very different scattering lengths for Sc ($b_{coh} = 12.29$ fm) and Ga ($b_{coh} = 7.288$ fm).²³ Moreover, neutrons are relatively more sensitive to low Z atoms, i.e. oxygen, allowing to determine its position with high accuracy.

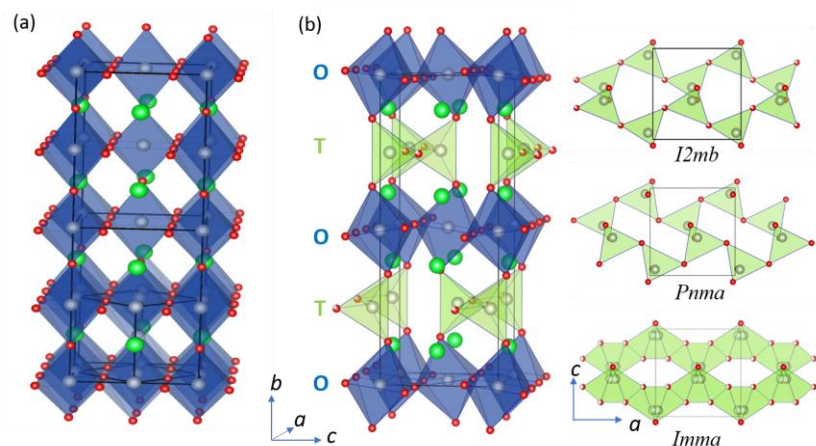


Figure 1. (a) Disordered perovskite and (b) brownmillerite structures. The disordered perovskite structure consists of a network of corner-sharing octahedra with oxygen vacancies randomly occupying the corner sites, whereas in brownmillerite, the oxygen vacancies form layers of alternating octahedral (O) and tetrahedral (T) chains. On the right, different orientations of the $(BO_4)_\infty$ -tetrahedral chains are shown, giving different possible space groups in brownmillerite type frameworks. Full ordering is achieved for both $I2mb$ and $Pnma$ space groups, while a superposition of both arrangements results, on an average scale, into split positions for the BO_4 tetrahedra, described within the $Imma$ space group.

2. Experimental

Synthesis

Polycrystalline Sr_2ScGaO_5 compounds were prepared by classical solid-state chemistry synthesis at high temperature. High purity $SrCO_3$ (99,995%, ALDRICH), Ga_2O_3 (99,99%, ALDRICH) and Sc_2O_3 (REacton 99,99% REO, ALFA AESAR) were thoroughly mixed and heated in air at $1200^\circ C$ for 48 h, with intermediate grinding, to obtain the brownmillerite phase (BM-SSGO in the following). Cubic phase (C-SSGO in the following) has been

obtained by heating the brownmillerite counterpart at 1500°C for several hours and then furnace cooling (about 5 °C/min) down at room temperature.

Neutron PDF Diffraction

Neutron total scattering data for both compounds was collected on the disorder materials diffractometer D4c at ILL (Grenoble, France) with an incident neutron wavelength $\lambda = 0.4989 \text{ \AA}$, covering a Q range between 0.35 and 23.6 \AA^{-1} , at different temperatures below and above the phase transition, i.e. RT, 250°C; 350°C, 450°C, 550°C, 650°C, 750°C, 850°C.

The reduction and merging of the raw neutron data to obtain the pair distribution function $G(r)$ was carried out using a software procedure developed at D4c. The fitting of the $G(r)$ was performed using the program PDFgui, a small-box modelling real-space 'Rietveld' refinement program.^{24, 25}

EXAFS

X-ray absorption spectroscopy (XAS) measurements at Ga K edge (10367 eV) were performed at beamline Spline BM25 of the European Synchrotron Radiation Facility (ESRF, Grenoble, France). The white beam was monochromatized by Si(111) double crystal monochromator and the harmonic rejection was performed by two silicon mirrors. Spectra were acquired in transmission configuration by ion chambers. The powder samples were hosted inside a reactor cell for in situ experiment in form of self-supported pellet with optimized X-rays path. Both samples, BM-SSGO and C-SSGO, were measured from RT up to 650°C at several temperatures and at least three spectra for each temperature were collected.

The extended X-ray absorption fine structure (EXAFS) region was acquired up to a photoelectron wave vector $k = 15 \text{ \AA}^{-1}$, while the range used in the data analysis is reported in the note of the Tables where the quantitative results are summarized.

Data reduction and analysis were performed by IFEFFIT package, phase and amplitudes of EXAFS signal for fit procedure were calculated by FEFF6 starting from the structural model.²⁶ The spectra collected at increasing temperature were analyzed by co-refinement fit strategy in order to reduce the number of free parameters and minimize the correlation across them.

3. Results

3.1 PDF analysis

Figure 2a-b shows the experimentally obtained neutron pair distribution functions $G(r)$ for both SSGO phases, the cubic perovskite (C-SSGO) and the orthorhombic brownmillerite (BM-SSGO), as a function of the temperature, on the 0.5 – 30 Å distance range.

In the view of the very different XPD patterns (see Figure S1), it is somehow intriguing to see the resemblance of both phases on a local length scale up to 8 Å, while above this value significant differences become directly evident.

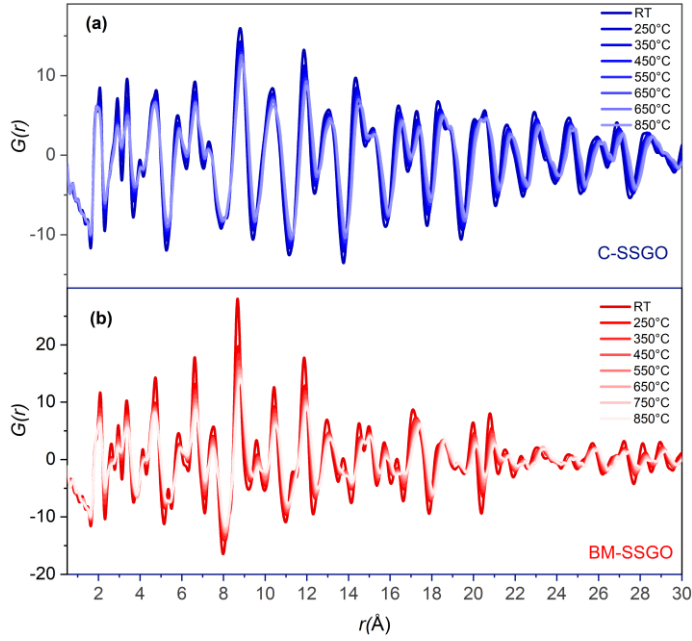


Figure 2: Experimentally obtained $G(r)$ data for (a) cubic (C-SSGO) and (b) orthorhombic (BM-SSGO) $\text{Sr}_2\text{ScGaO}_5$ as collected at different temperatures (RT, 250°C, 350°C, 450°C, 550°C, 650°C, 750°C, 850°C).

3.1.1 Orthorhombic phase

The average brownmillerite-type structure of $\text{Sr}_2\text{ScGaO}_5$ (BM-SSGO), as determined by neutron powder diffraction, is described in the $I2mb$ space-group at ambient temperature, ($a = 5.6971(1) \text{ \AA}$, $b (\text{Å}) = 15.1295(2) \text{ \AA}$, $c (\text{Å}) = 5.9074(1) \text{ \AA}$), showing complete ordering of Sc^{3+} and Ga^{3+} on octahedral and tetrahedral sites, respectively, while all the $(\text{GaO}_4)_\infty$ -tetrahedral chains are completely ordered. Above 300°C these chains become disordered and the space group turns into $Imma$.¹⁴ We note that the structural changes between $I2mb$ and $Imma$ are very subtle also because the conditions for reflections are identical in both cases. The symmetry relations result, however, into a different coordination for the ScO_6 octahedra: for $Imma$ the coordination of Sc shows two symmetry equivalent oxygen atoms, while in three distinct oxygen sites exist for $I2mb$. For Ga atoms, 3 crystallographic different oxygen

positions are present for both space groups (see Figure 3). Thus, the difference given by the coordination of the ScO_6 octahedra would also allow to revisit here discussions of the structural changes through the phase transition on a more local level.

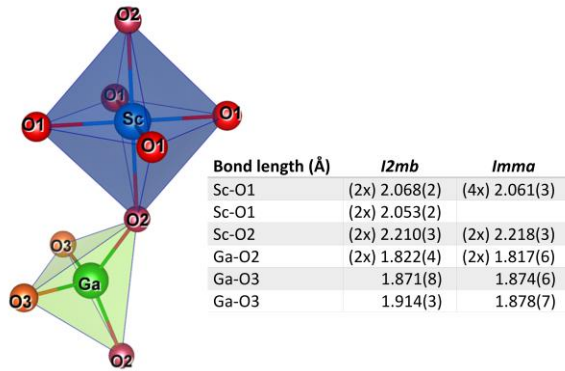


Figure 3: Schematic view of ScO_6 octahedra and GaO_4 tetrahedra in the $\text{Sr}_2\text{ScGaO}_5$ average brownmillerite-type structure as obtained from NPD refinements and corresponding bond lengths for the *I2mb* and *Imma* space group.¹⁴ ~~In the *Imma* space group, Ga is in a split position but here for sake of clarity we considered only one position.~~

The BM-SSGO neutron PDF was fitted using both models over different r -ranges, using the PDFgui software (Table 1). In the low r -space ($0.5 \text{ \AA} \leq r \leq 7 \text{ \AA}$) the PDF data nicely fit for the *I2mb* symmetry (fitting residuals R_w around 6%) for all explored temperatures ($30^\circ\text{C} \leq T \leq 850^\circ\text{C}$), which is not really the case for refinements in *Imma*. Even above the structural phase transition, where *Imma* is supposed to be the correct description, the fit results are by far less satisfactory compared to the fitting in *I2mb* (see Table 1). Moving away from the short-range distance, i.e. for $r \geq 7 \text{ \AA}$, where the PDF data result in a more averaged description, refinements in *Imma* and *I2mb* become very close in quality and almost indistinguishable at higher temperatures. The important message is therefore that on a very

local scale, the structure of the brownmillerite $\text{Sr}_2\text{ScGaO}_5$ phase is better described by the lower symmetry $I2mb$, independently of the temperature.

Table 1: Fitting residuals (R_w)* of the PDF refinements of the orthorhombic BM-SSGO over different r -ranges with two structural models ($I2mb$ and $Imma$), at the different measuring temperatures.

		R_w (%) for $0.5 < r < 7 \text{ \AA}$		R_w (%) for $7 < r < 30 \text{ \AA}$	
Space Group Temperature	$I2mb$	$Imma$	$I2mb$	$Imma$	
	RT	6.0	20.0	12.0	15.0
250 °C	7.0	18.0	14.0	15.0	
350 °C	7.6	17.0	14.6	14.0	
450 °C	7.1	17	14.6	14.0	
550 °C	6.5	16	14.5	14.0	
650 °C	6.2	14.0	15.0	14.0	
750 °C	6.1	15.0	15.1	14.1	
850 °C	6.5	15.2	16.0	15.0	

*The weighted R-value is calculated as follows: $R_w = \left\{ \frac{\sum w_i (G_i^{obs} - G_i^{calc})^2}{\sum w_i (G_i^{obs})^2} \right\}^{1/2}$, where G_i^{obs} and G_i^{calc} are the experimental and calculated PDFs, respectively, and w_i are the weighting factors.

As an example, the fitting results of the RT data of BM-SSGO over the whole r -range considering the $I2mb$ space group, are shown in Figure 4. Attempts to fit the whole data in $Imma$ lead to refinements with significant differences between the experimental and calculated data (see Fig. S2). The fit quality for the $7 \text{ \AA} \leq r \leq 30 \text{ \AA}$ data yielded a reliability

factor $R_w = 15.0\%$, while the data for $r \leq 7 \text{ \AA}$ yielded a value of $R_w = 20.0\%$, presenting a significant difference compared to 12.0% and 6.0% using *I2mb*. All structural parameters obtained at room temperature are listed in Table S1 and compared to structural refinements by the Rietveld method previously reported.¹⁴ It should be noted that both methods, the PDF and Rietveld refinements in *I2mb*, yield analogous results, also suggesting that the two structural approaches are fully comparable.

It thus becomes clear that below the phase transition the structure corresponds to an oxygen ordered brownmillerite adapting the space group *I2mb*, at long and local length scale, which is however contradictory to what is reported in ref.²⁷.

For temperature above $300 \text{ }^\circ\text{C}$, the PDF analysis of the diffraction data does not permit to distinguish between the *Imma* and *I2mb* space group at longer length scale, while the *I2mb* symmetry is retained on a local level for the whole temperature range (Table 1). This is illustrated in Figure S3 showing the PDF-refinement at $550 \text{ }^\circ\text{C}$ using the *I2mb* and *Imma* model in the short ($0.5 \text{ \AA} \leq r \leq 7 \text{ \AA}$) and average-long distance range $r \geq 7 \text{ \AA}$, respectively. The evolution of the lattice parameters as well as the isotropic displacement factors U_{iso} , as obtained by PDF refinements at longer length scales are given as a function of temperature in Table S2 and Fig. 5a-b. They are fully consistent with the structural parameters found by neutron powder diffraction data Rietveld refinements¹⁴, which are indicated as crosses in Figure 5a-b. The bond lengths and the U_{iso} , extracted from the $0.5\text{-}7 \text{ \AA}$ range PDF fitting, are shown in Figure 9.

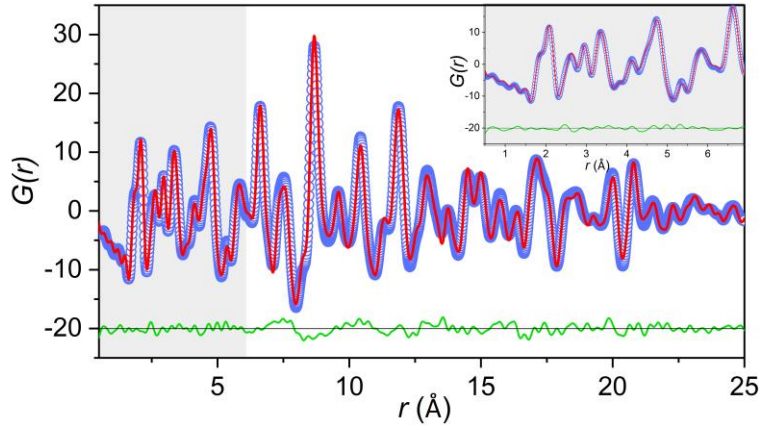


Figure 4: PDFgui refinement (at room temperature) for orthorhombic BM-SSGO from $r = 0.5$ to 30 \AA with the $I2mb$ model. In the inset the short-range $G(r)$ is zoomed. Blue open circles are the experimentally PDF data, red line the profile fitting while the green line is the difference between observed and calculated data. The quality of fit is satisfactory, giving $R_w = 12.0\%$.

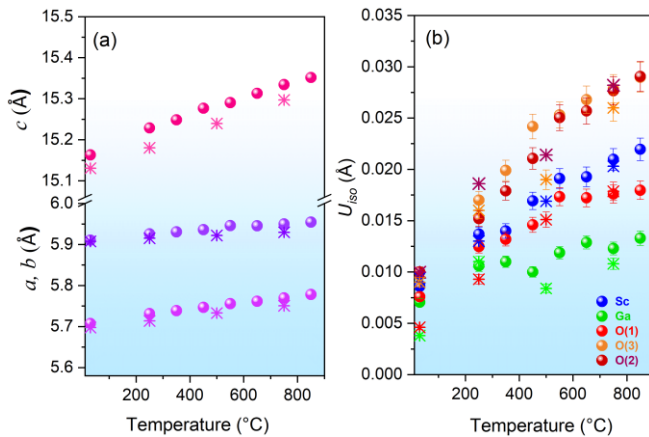


Figure 5: Evolution of the lattice parameters (a) and of the displacements factors (b) as a function of the temperature as found from refinement of the pair distribution function in the long distance range ($7 \text{ \AA} \leq r \leq 30 \text{ \AA}$). For comparison, the lattice constants as well as the displacement factors determined from our previous diffraction experiments are also reported (stars).¹⁴ Error bars are within the respective symbol sizes. For comparison, the U_{iso} as obtained on a local scale on the BM-SSGO, are reported in Figure 8 (left).

3.1.2 Cubic SSGO

When brownmillerite-type $\text{Sr}_2\text{ScGaO}_5$ is heated up to 1500°C , the cubic polymorph is obtained and can be stabilized as a metastable phase at ambient temperature via slow furnace cooling, suggesting that both phases are energetically close.²⁸ From X-ray and NPD the cubic symmetry is directly evident showing a lattice parameter of $a = 3.9932(1) \text{ \AA}$ (Figure S1).^{15, 16} From the neutron diffraction data, it is noticeable that the background is quite modulated, indicating diffuse scattering due to some short-range order. As it is not evidenced by X-ray diffraction, this is supposed to be associated to oxygen vacancy ordering/correlations. Short-range oxygen ordering related to the oxygen deficiency in $\text{Sr}(\text{Sc}/\text{Ga})\text{O}_{2.5}\square_{0.5}$ (\square = vacancy) and the formation of ScO_6 and GaO_4 polyhedra instead of an average 5-fold coordination has already been suggested in ref.^{15, 16}.

Figure 6 shows the nearest neighbor range ($1 \text{ \AA} < r < 4.5 \text{ \AA}$) of the experimental pair distribution function $G(r)$ obtained by neutron diffraction for both, the C-SSGO and BM-SSGO at room temperature. From the average cubic perovskite structure model in $Pm-3m$ and a lattice parameter of $a = 3.9932(1) \text{ \AA}$, interatomic distances can be calculated to (Sc/Ga) – O at 1.99 \AA , Sr-O at 2.8215 \AA , (Sc/Ga)-Sr at 3.4554 \AA and Sr-Sr at 3.99 \AA and are indicated by a dashed black line. It thus becomes directly obvious that for the C-SSGO phase, the first two peaks corresponding to (Sc/Ga)-O and Sr-O distances, which would be expected to be as a single one for the average perovskite, appear both to be more complex and very analogous to the BM-SSGO counterpart in the experimental data. With that it becomes understandable that attempts to fit the experimental data with the cubic $Pm-3m$ model yielded only very poor results in the low- r region. As the cubic model fails to describe the real local structure, we proceeded with refinements at short length scale from 0.5 to 5 \AA , considering the vacancy ordered brownmillerite phase in $I2mb$. Attempts to refine in $Imma$ yielded quite poor results

and are not further considered in the following discussion. Because of the important number of atomic degrees of freedom for this model, the refinement strategy implied to fix at first the lattice parameters and **atomic coordinates** to those obtained by X-ray/neutron diffraction for the BM-SSGO¹⁴ while refining the thermal displacements only. In a second step, lattice parameters were then allowed to refine together with the atomic positions, resulting in very good fit results with $R_w = 6.0\%$. Moving away from the short-range scale beyond $r > 5 \text{ \AA}$, the experimental data don't match any more with the brownmillerite framework but approach the average cubic model. Refinements in the $Pm-3m$ model and $r > 5 \text{ \AA}$ give quite satisfactory agreement values of $R_w = 15.0\%$, indicating only minor deviation from the average perovskite structure at medium and longer length scales. Figure 7 shows the PDF fit for C-SSGO, taking into account the $I2mb$ model in the short length range, and the cubic $Pm-3m$ model at medium and high distance range.

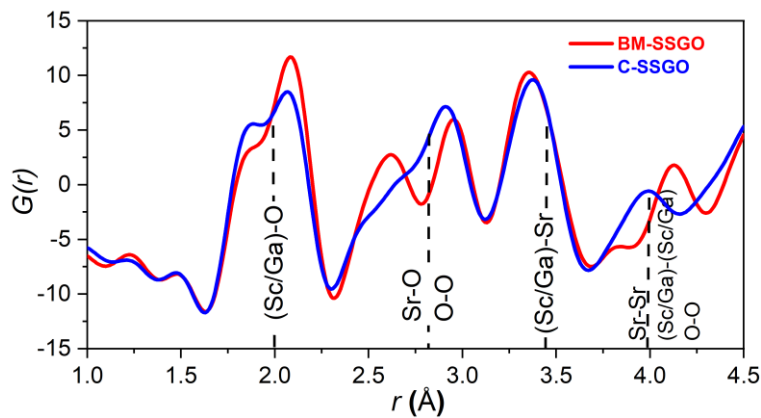


Figure 6: Low- r region of neutron PDF data at room temperature of the cubic (C-SSGO, blue line) and orthorhombic phase (BM-SSGO, red line). For comparison the single nearest interatomic distances calculated for the cubic perovskite are also reported (black dashed lines).

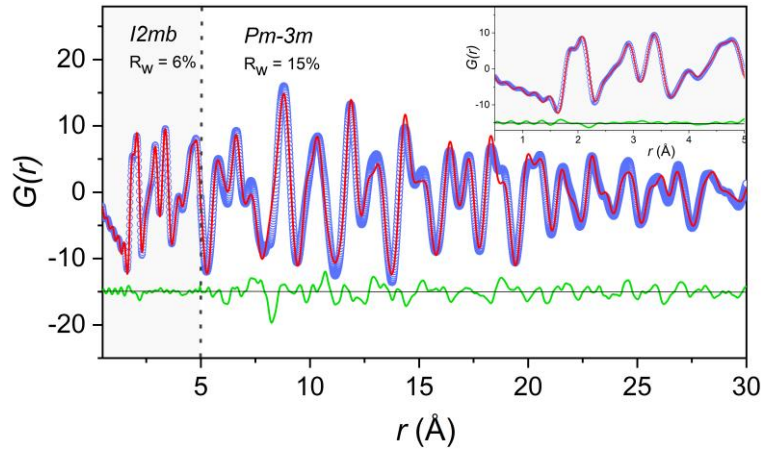


Figure 7: Long and short r -range $G(r)$ obtained for C-SSGO, refined with the $I2mb$ structure in the low r region ($0.5 \text{ \AA} < r < 5 \text{ \AA}$) (zoomed in the inset) while the in the medium and high r range data are refined with the average cubic structure $Pm-3m$.

Corresponding structural data are reported for the whole temperature range in Tables S3 and S4 for short and long-range distances respectively. Unlike the average perovskite structure, the oxygen ordered brownmillerite type framework could be clearly evidenced by PDF analysis to be present, at least on a local length scale. This does, however, not imply an accurate structural description comprising details for the twisting directions of the tetrahedral chains. It evidences nevertheless a layer sequence of alternating $\text{ScO}_6/\text{GaO}_4$ units, confirming B-cation ordering at least on a shorter length scale. This is much better evidenced with neutron diffraction as the contrast between Sc and Ga is increased compared to X-rays.

Despite the structural resemblance on a local length scale for C-SSGO and BM-SSGO, there exist nevertheless some structural differences, especially concerning isotropic displacement factors (U_{iso}), shown in Figure 8, respectively. Generally, they are not only lower in case of C-SSGO, but they are also found to stay practically unchanged for the whole T-range from RT to 850°C .

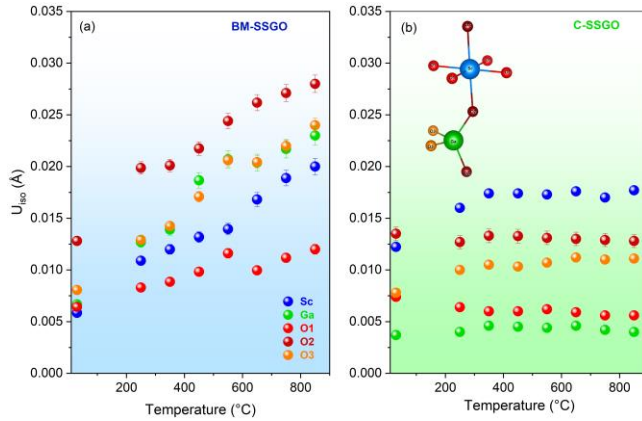


Figure 8: Displacement factors U_{iso} obtained through PDF fit in the short length scale ($r < 5$ Å), against the $I2mb$ space group, at for the brownmillerite BM-SSGO (on the left) and the cubic perovskite C-SSGO (on the right) as a function of temperature.

In the same way, the bonding lengths for C-SSGO (Fig. 9b) extracted from the PDF fitting in $I2mb$ at local r range are quite comparable to the brownmillerite counterpart (Fig. 9a). The only difference concerns the Ga-O(3) distances, i.e. all equatorial oxygen around Ga, which are slightly smaller compared to the BM-SSGO over the whole temperature range.

The almost constant values for the displacement factors found for C-SSGO indicate that GaO_4 tetrahedra as well as ScO_6 octahedra are behaving quite rigidly. A simplified sketch of the local environment for both polyhedra is given in Fig. 9d, corresponding to the length scale taken into account for the data fitting. It indicates an enlarged ScO_6 octahedron, while the GaO_4 tetrahedron gets reduced accordingly. This allows both B-cations, Sc and Ga, to reach their typical oxygen distances found for the brownmillerite structure type, i.e.

(2.22/2.06/2.06) Å and (1.91/1.87/1.81) Å, respectively. Thereby the sum of the Sc-O(2) and

Ga-O(2) distances in C-SSGO (Fig 9c) yields 4.03 Å , very close to the cubic unit cell parameter of 4 Å. The same holds for the respective equatorial oxygen atoms, i.e. Sc-O(1)+Ga(O3), yielding 3.95 Å as an average. The corresponding lattice mismatch of less than 2% is thus relatively small and may explain why the transformation from the average cubic perovskite to brownmillerite-type structure gets somehow inhibited, allowing to obtain C-SSGO even during slow furnace cooling. We note that the Sc-O and Ga-O distances in the Brownmillerite structure in $I2mb$ are almost identical to the values found here, although the octahedra show a tilting around $[100]$ of about 11° . The thus engendered error is however small and reduces the total effective length compared to a linear Sc-O-Ga configuration by less than 1% only.

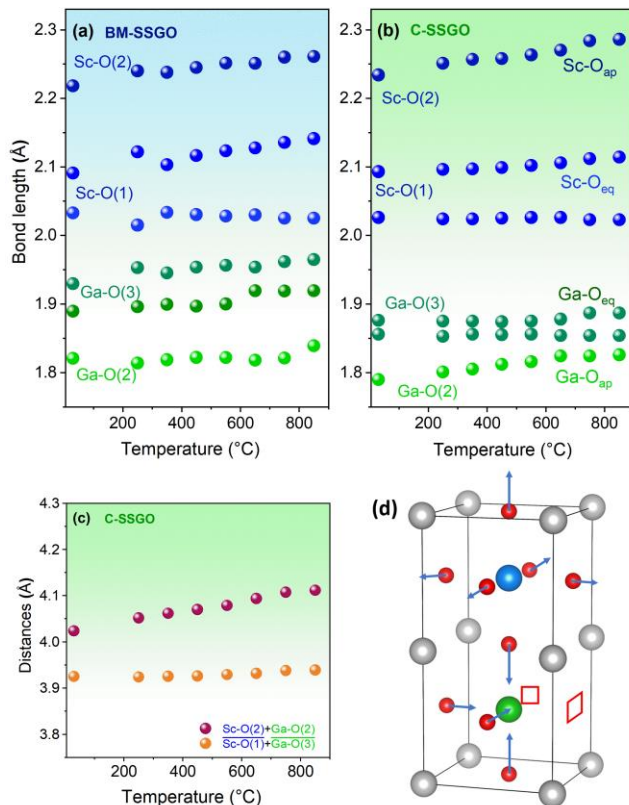


Figure 9: (a) Bond lengths on the local scale in the brownmillerite BM-SSGO and (b) in the cubic C-SSGO as a function of the temperature, as determined by PDFgui fitting (through the

I2mb space group). (c) Temperature evolution of sum Sc-O_{ap} and Ga-O_{ap} distances and of the respective average distances between Ga and Sc towards their equatorial atoms; (d) Simplified scheme of the local environment for GaO₄ tetrahedra and ScO₆ octahedra in C-SSGO.

3.2 EXAFS: Ga K-Edge

The room temperature EXAFS spectra ($|FT|$ and $Imm(FT)$) of both, the brownmillerite BM-SSGO and perovskite C-SSGO phases are shown in real and k space in Figure 10 and Figure S4, respectively. Both spectra are characterized by a very similar first peak around 1.4 Å attributed to the nearest coordination Ga-O shells (all FT plots are not phase-corrected, so coordination shell peaks are shifted to lower r by approximately 0.4 - 0.5 Å), suggesting a very close bonding environment for both the cubic and orthorhombic SSGO phases. This implies that Ga in the cubic C-SSGO has the same coordination as compared to the brownmillerite counterpart, i.e. Ga in tetrahedral and consequently Sc in octahedral coordination, as already suggested by neutron PDF analysis reported above. The second peak observed in both samples at around 3 Å is the convolution of several Single Scattering and Multiple Scattering contributions, including two and three body configurations involving Ga, Sr, Sc and O atoms. All the Single Scattering paths contributing to this peak are reported in Table S6. This peak is quite well defined and intense for BM-SSGO while it is broad and weaker for C-SSGO, probably reflecting different degree of order of its structure.

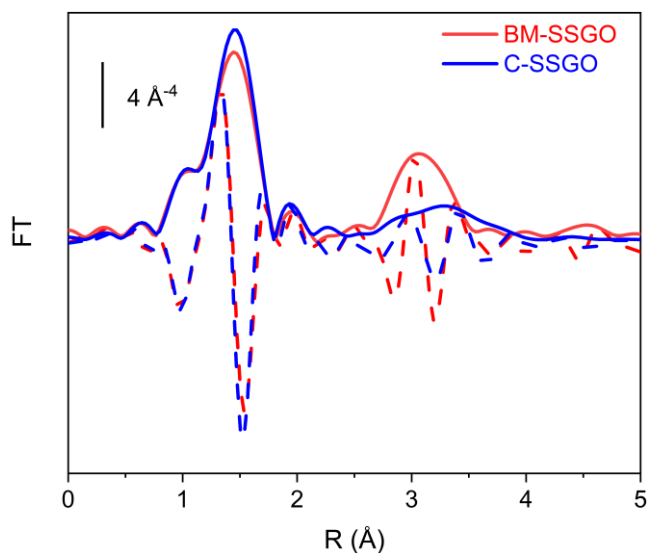


Figure 10: Fourier Transform of $k^3\text{-}\chi(k)$ EXAFS spectra, no phase corrected, of brownmillerite BM-SSGO (red curve) and perovskite C-SSGO (blue) samples measured at RT. Both $|FT|$ (bold lines) and $Imm(FT)$ (dashed lines) are reported.

To verify the local structure of both samples, the spectra at RT were firstly analyzed by fitting the first peak with a simple model including only one Ga-O contribution. The coordination number extracted by EXAFS analysis resulted quite close to 4 for both phases, indicating a tetrahedral coordination of Ga as suggested by PDF data, reported in the previous paragraph. The complete details of the data analysis are provided in Table S5.

Starting from these results, the analysis was extended to the second contribution considering the orthorhombic $I2mb$ structure. The complexity of the structure implies to include several paths contributions to reproduce the EXAFS signal during the fitting procedure. In order to minimize the correlation of the free parameters and to have a robust output, few parameters were optimized: (i) one amplitude reduction factor S_0^2 , (ii) 2 Debye-Waller factors: one for the oxygen (σ^2_O) atoms and one for the others (σ^2_{other}); (iii) one parameters for the optimization of bond distances alpha; (iv) one parameters for absorption energy E_0 . The results of the fit of the

free parameters and the list of Single Scattering paths together with their structural information are reported in Table 2 and Table S6, respectively. The quality of the fit of both samples can be appreciated in Figure 11a-b and Figure S3 in R space and k space, respectively.

Table 2: Free parameters of the extended fit up to 3.8 Å performed at RT on the brownmillerite (BM-SSGO) and cubic (C-SSGO) Sr₂ScGaO₅ samples

	BM-SSGO	C-SSGO
CN	1.84(2)	1.76(4)
$\sigma^2_{\text{O}} (\text{Å}^2)$	0.0024(4)	0.0012(5)
$\sigma^2_{\text{others}} (\text{Å}^2)$	0.0082(4)	0.018(2)
alpha ^a	0.0044(12)	-0.0017(27)
E ₀ (eV)	4.4(3)	5.5(1)
S ₀ ²	0.93(4)	0.88(6)
R _{factor}	0.0058	0.00135

^a bond distance: $R=R_{\text{eff}}+R_{\text{eff}}*\text{alpha}$, Fitting range: $\Delta k=2.5-12.7 \text{ Å}^{-1}$; $\Delta r=1-3.8 \text{ Å}$; S₀² is the amplitude reduction factor, E₀ is the threshold energy. All the distances R_{eff} are reported in Table S6

For the brownmillerite phase BM-SSGO, the quality of the fit is very good for the whole considered EXAFS region, with excellent agreement between experimental and modelled data (Figure 11a). The values of the optimized parameters, as reported in Tables 2-S7, are also in an acceptable range and associated at the same time to small errors. On the base of these results it can be concluded that the *I2mb* model considered in the fit matches well with the spectroscopy data and is able to reproduce the local environment of Ga in SSGO brownmillerite. For the perovskite phase C-SSGO, the first peak is perfectly reproduced by the *I2mb* model. The second peak centered at 3 Å is, however, not completely fitted within this model (Figure 11b). The Debye-Waller value, σ^2_{others} (0.018(2)) is also larger than that of the brownmillerite counterpart

(0.0082(4)), suggesting an higher degree of disorder. However, a careful inspection of the data, and in particular the imaginary part of FT (Figure 11b) and of the spectra in k space (Figure S4b), shows that all features of the modelled signal are matching the correct position of the experimental data while there is only a lacking in their relative intensity. This observation supports thus the hypothesis that the average perovskite phase is affected by different degree of disorder but its local structure is still well represented by $I2mb$ symmetry, comforting the results obtained by PDF analysis.

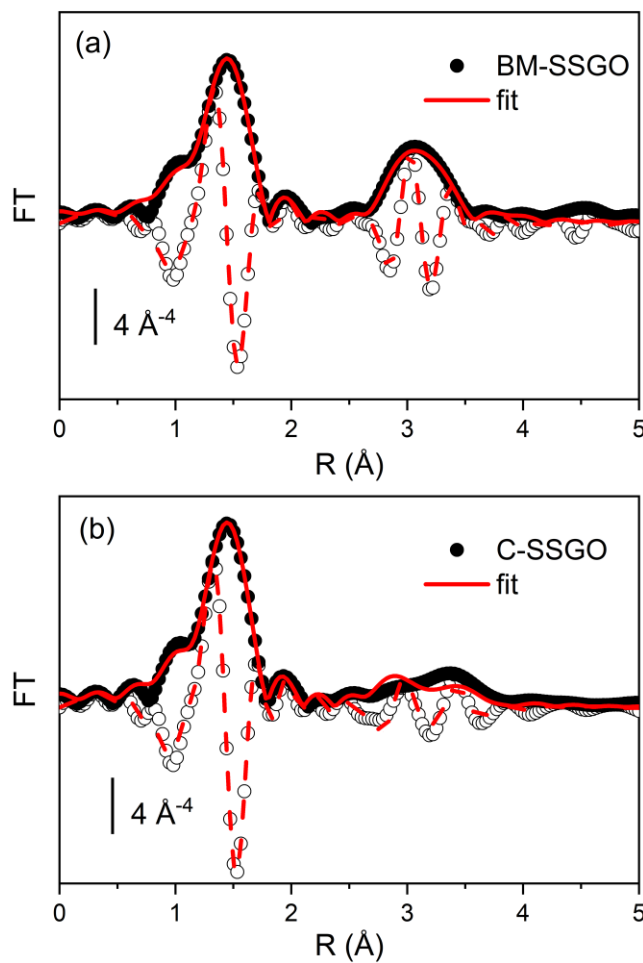


Figure 11: Fourier Transform of $k^3\text{-}\chi(k)$ EXAFS spectra, no phase corrected, of experimental data (scattered points) and fit (red curves) performed on samples BM-SSGO (part a) and C-SSGO (part b) collected at RT. Full and black empty dots are experimental $|FT|$ and $Imm(FT)$, respectively, while continuous and dashed red lines are the corresponding fits.

After this RT analysis, suggesting a four-fold coordination of Ga on a local scale, the evolution of the local order as a function of temperature has been investigated by first shell analysis.

All spectra were collected at increasing temperature and analyzed simultaneously considering the *I2mb* structure. The first shell is composed by three different Ga-O contributions at slightly different bond lengths, while the shortest contribution shows a twofold coordination number, (see Table S6, second and fourth column, for more details). These paths were included in the fit, optimizing only one Debye-Waller factor for each temperature. The other parameters, i.e. the optimization of the bond length *beta*, the amplitude reduction factor S_0^2 and the absorption energy E_0 , were in common for the whole data set. The results of the analysis have been reported in Table S6; the Debye Waller (DW) factors extracted by the fit are reported in Figure 12 as a function of the temperature. It is clear that for the cubic C-SSGO, the DW factors σ^2 are smaller than those of the brownmillerite counterpart, confirming the results of the neutron pair distribution function analysis.

It is worthwhile to note that the DW factor derived from EXAFS (σ^2), called also “disorder factor”, represents the spreading of the interatomic distances around each site, thus it represents the parallel mean square relative displacement (MSRD), i.e. it is a measure of the variations of two atoms relative each other along the bond direction.²⁹ Considering the first shell, σ^2 are much smaller than the Debye Waller obtained by neutron diffraction^{14, 16}, representative of the uncorrelated mean square displacement (MSD), for both the cubic and orthorhombic phases. Smaller σ^2 are possible if Ga and O are at least partially in phase. The difference between MSD and MSRD is thus consistent with a strong in-phase motion of the neighboring Ga-O atoms along the bond directions. Together with the fact that displacement factors found by PDF analysis are pretty low, this underlines the quite rigid body behavior of the GaO₄ tetrahedra.

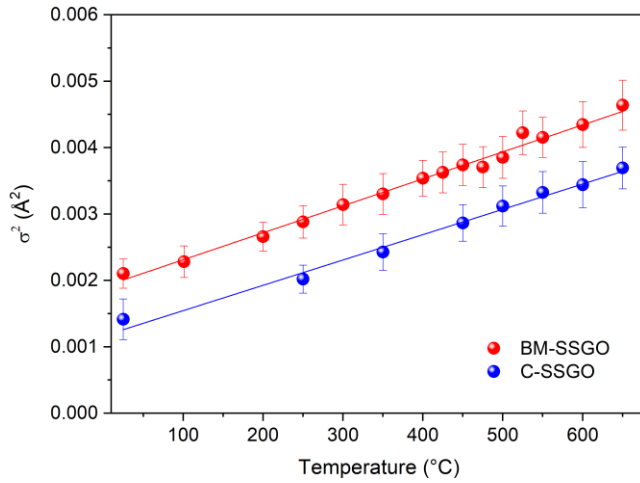


Figure 12: Evolution of the EXAFS Debye-Waller factors as a function of temperature as obtained from the first shell analysis performed on the brownmillerite BM-SSGO (red curve) and perovskite C-SSGO (blue curve) $\text{Sr}_2\text{ScGaO}_5$.

Conclusion

The local structures of $\text{Sr}_2\text{ScGaO}_5$ polymorphs with brownmillerite and perovskite type structure have been investigated, combining neutron pair distribution function and EXAFS analysis. Based on our NPD structure refinements published elsewhere, both methods yielded additional and complementary structural information. Most surprisingly we could evidence the space group for the brownmillerite phase being $I2mb$ on a local length scale ($r < 7\text{\AA}$) over the whole explored T-range (RT- 800 °C). This looks at first sight contradictory compared to the disordered $1D\text{-(GaO}_4)_\infty$ tetrahedral chains in $Imma$, as set from Rietveld refinement of NPD data above 300°C. It also suggests that the tetrahedral chains are *not* dynamically disordered, but the split position found for the GaO_4 tetrahedra are presumably related to an inter-tetrahedral layer correlation problem, resulting into artificially superimposed tetrahedral

switching positions. It thus contradicts the current understanding of oxygen diffusion along the 1D vacancy channels, activated by a dynamical switching of the tetrahedral chains above the $I2mb/Imma$ phase transition, and which is currently under further investigation.

For the oxygen deficient cubic perovskite SSGO, the presence of brownmillerite type entities was clearly approved on a local length scale by both, neutron PDF and EXAFS at the Ga-edge. It confirms the existence of GaO_4 tetrahedra as well as ScO_6 octahedra as the basic polyhedra to constituting this apparently *average* network as seen by classical diffraction. It also implies, supported by the double peak structure of the $G(r)$ function, the formation of relaxed Sc-O and Ga-O distances which on an average scale measure around 2.15Å and 1.85Å respectively. This information is not as such directly available from NPD refinements. Further on, neutron PDF and EXAFS studies evidenced significantly reduced displacement factors compared to the brownmillerite phase for the whole T-range, directly underlining the rigid body behavior of the GaO_4 tetrahedra, and consequently for the ScO_6 octahedra. It becomes thus clear that the retention of the brownmillerite type framework, i.e. a layer sequence of $[ScO_6/GaO_4]$ entities on a local length scale, conditions the formation of short-range correlations of the oxygen vacancies together with B-cation ordering. The rather small displacement factors for the GaO_4 tetrahedra suggest, however, a pretty static conformation. The existence of brownmillerite nano-domains has been discussed analogously for the cubic $SrFeO_{2.5}$ above 830°C following Mössbauer spectroscopy, i.e. shortly after attaining the cubic perovskite structure as seen by diffraction methods.³⁰ While a facile change in the coordination of Fe allows an easy dynamic rearrangement of these domains, and thus reinforcing oxygen diffusion, this looks impractical for C-SSGO related to its rigid body behavior. A better understanding of what type of cross-linking network of brownmillerite type nano-domains in C-SSGO increases oxygen ion conductivity by more than one order of magnitude compared to the 1D oxygen vacancy channels existing in the pure brownmillerite framework is now under investigation.^{16, 31}

ASSOCIATED CONTENT

Supporting Information

The following files are available free of charge:

XRD and NPD diffraction patterns, Structural data obtained by PDF analysis, EXAFS spectra and fitting parameters (PDF)

AUTHOR INFORMATION

Corresponding Author

* monica.ceretti@umontpellier.fr

Present Address

† Maastricht Science Programme (MSP), Kapoenstraat 2, 6211 KW Maastricht, The Netherlands

ACKNOWLEDGMENT

The authors thank the beam line SpLINE at the European Synchrotron Facility and the Institut Laue Langevin (Grenoble, France) for the allocation of beam time. Neutron diffraction data are available from DOI: 10.5291/ILL-DATA.6-06-480.

REFERENCES

1. Abakumov, A. M.; Alekseeva, A. M.; Rozova, M. G.; Antipov, E. V.; Lebedev, O. I.; Van Tendeloo, G. Ordering of tetrahedral chains in the Sr₂MnGaO₅ brownmillerite. *J. Solid State Chem.* **2003**, 174 (2), 319-328.

2. Abakumov, A. M.; Rozova, M. G.; Pavlyuk, B. P.; Lobanov, M. V.; Antipov, E. V.; Lebedev, O. I.; Van Tendeloo, G.; Ignatchik, O. L.; Ovtchenkov, E. A.; Koksharov, Y. A.; Vasil'ev, A. N. Synthesis, Crystal Structure, and Magnetic Properties of a Novel Layered Manganese Oxide $\text{Sr}_2\text{MnGaO}_{5+\delta}$. *J. Solid State Chem.* **2001**, 160 (2), 353-361.
3. Hadermann, J.; Abakumov, A. M.; D'Hondt, H.; Kalyuzhnaya, A. S.; Rozova, M. G.; Markina, M. M.; Mikheev, M. G.; Tristan, N.; Klingeler, R.; Buchner, B.; Antipov, E. V. Synthesis and crystal structure of the $\text{Sr}_2\text{Al}_{1.07}\text{Mn}_{0.93}\text{O}_5$ brownmillerite. *J. Mater. Chem.* **2007**, 17 (7), 692-698.
4. Shaula, A. L.; Pivak, Y. V.; Waerenborgh, J. C.; Gaczynski, P.; Yaremchenko, A. A.; Kharton, V. V. Ionic conductivity of brownmillerite-type calcium ferrite under oxidizing conditions. *Solid State Ionics* **2006**, 177 (33-34), 2923-2930.
5. Wu, J. W.; Wang, J.; Liu, G.; Wu, Y. J.; Liu, X. Q.; Chen, X. M. Giant room-temperature magnetodielectric coupling in spark plasma sintered brownmillerite ceramics. *Appl. Phys. Lett.* **2014**, 105 (22), 222906.
6. Goodenough, J. B.; Ruiz-Diaz, J. E.; Zhen, Y. S. Oxide-ion conduction in $\text{Ba}_2\text{In}_2\text{O}_5$ and $\text{Ba}_3\text{In}_2\text{MO}_8$ (M=Ce, Hf, or Zr). *Solid State Ionics* **1990**, 44 (1), 21-31.
7. Chen, C.-F.; King, G.; Dickerson, R. M.; Papin, P. A.; Gupta, S.; Kellogg, W. R.; Wu, G. Oxygen-deficient BaTiO_{3-x} perovskite as an efficient bifunctional oxygen electrocatalyst. *Nano Energy* **2015**, 13, 423-432.
8. Petrie, J. R.; Jeen, H.; Barron, S. C.; Meyer, T. L.; Lee, H. N. Enhancing Perovskite Electrocatalysis through Strain Tuning of the Oxygen Deficiency. *J. Am. Chem. Soc.* **2016**, 138 (23), 7252-7255.
9. Parsons, T. G.; D'Hondt, H.; Hadermann, J.; Hayward, M. A. Synthesis and Structural Characterization of $\text{La}_{1-x}\text{AxMnO}_{2.5}$ (A = Ba, Sr, Ca) Phases: Mapping the Variants of the Brownmillerite Structure. *Chem. Mater.* **2009**, 21 (22), 5527-5538.
10. King, G.; Thompson, C. M.; Luo, K.; Greedan, J. E.; Hayward, M. A. Identifying the local structural units in $\text{La}_{0.5}\text{Ba}_{0.5}\text{MnO}_{2.5}$ and $\text{BaY}_{0.25}\text{Fe}_{0.75}\text{O}_{2.5}$ through the neutron pair distribution function. *Dalton Transactions* **2017**, 46 (4), 1145-1152.
11. Nemudry, A.; Weiss, P.; Gainutdinov, I.; Boldyrev, V.; Schollhorn, R. Room temperature electrochemical redox reactions of the defect perovskite $\text{SrFeO}_{2.5+x}$. *Chem. Mater.* **1998**, 10 (9), 2403-2411.
12. Maity, A.; Dutta, R.; Penkala, B.; Ceretti, M.; Letrouit-Lebranchu, A.; Chernyshov, D.; Perichon, A.; Piovano, A.; Bossak, A.; Meven, M.; Paulus, W. Solid-state reactivity explored in situ by synchrotron radiation on single crystals: from $\text{SrFeO}_{2.5}$ to SrFeO_3 via electrochemical oxygen intercalation. *J. Phys. D: Appl. Phys.* **2015**, 48 (50), 504004.
13. Le Toquin, R.; Paulus, W.; Cousson, A.; Prestipino, C.; Lamberti, C. Time-Resolved in Situ Studies of Oxygen Intercalation into $\text{SrCoO}_{2.5}$, Performed by Neutron Diffraction and X-ray Absorption Spectroscopy. *J. Am. Chem. Soc.* **2006**, 128 (40), 13161-13174.
14. Corallini, S.; Ceretti, M.; Silly, G.; Piovano, A.; Singh, S.; Stern, J.; Ritter, C.; Ren, J.; Eckert, H.; Conder, K.; Chen, W.-t.; Chou, F.-C.; Ichikawa, N.; Shimakawa, Y.; Paulus, W. One-Dimensional Oxygen Diffusion Mechanism in $\text{Sr}_2\text{ScGaO}_5$ Electrolyte Explored by Neutron and Synchrotron Diffraction, ^{17}O NMR, and Density Functional Theory Calculations. *The Journal of Physical Chemistry C* **2015**, 119 (21), 11447-11458.
15. Ceretti, M.; Corallini, S.; Paulus, W. Influence of Phase Transformations on Crystal Growth of Stoichiometric Brownmillerite Oxides: $\text{Sr}_2\text{ScGaO}_5$ and $\text{Ca}_2\text{Fe}_2\text{O}_5$. *Crystals* **2016**, 6 (11), 146.
16. Corallini, S.; Ceretti, M.; Cousson, A.; Ritter, C.; Longhin, M.; Papet, P.; Paulus, W. Cubic $\text{Sr}_2\text{ScGaO}_5$ Perovskite: Structural Stability, Oxygen Defect Structure, and Ion Conductivity Explored on Single Crystals. *Inorg. Chem.* **2017**, 56 (5), 2977-2984.

17. Chernov, S. V.; Dobrovolsky, Y. A.; Istomin, S. Y.; Antipov, E. V.; Grins, J.; Svensson, G.; Tarakina, N. V.; Abakumov, A. M.; Van Tendeloo, G.; Eriksson, S. G.; Rahman, S. M. H. $\text{Sr}_2\text{GaScO}_5$, $\text{Sr}_{10}\text{Ga}_6\text{Sc}_4\text{O}_{25}$, and $\text{SrGa}_{0.75}\text{Sc}_{0.25}\text{O}_{2.5}$: a Play in the Octahedra to Tetrahedra Ratio in Oxygen-Deficient Perovskites. *Inorg. Chem.* **2012**, 51 (2), 1094-1103.
18. Ramezanipour, F.; Greedan, J. E.; Siewenie, J.; Proffen, T.; Ryan, D. H.; Grosvenor, A. P.; Donaberger, R. L. Local and Average Structures and Magnetic Properties of $\text{Sr}_2\text{FeMnO}_{5+y}$, $y = 0.0, 0.5$. Comparisons with $\text{Ca}_2\text{FeMnO}_5$ and the Effect of the A-Site Cation. *Inorg. Chem.* **2011**, 50 (16), 7779-7791.
19. Ramezanipour, F.; Greedan, J. E.; Cranswick, L. M. D.; Garlea, V. O.; Siewenie, J.; King, G.; Llobet, A.; Donaberger, R. L. The effect of the B-site cation and oxygen stoichiometry on the local and average crystal and magnetic structures of $\text{Sr}_2\text{Fe}_{1.9}\text{M}_{0.1}\text{O}_{5+y}$ ($M = \text{Mn, Cr, Co}$; $y = 0, 0.5$). *J. Mater. Chem.* **2012**, 22 (19), 9522-9538.
20. Ramezanipour, F.; Greedan, J. E.; Siewenie, J.; Donaberger, R. L.; Turner, S.; Botton, G. A. A Vacancy-Disordered, Oxygen-Deficient Perovskite with Long-Range Magnetic Ordering: Local and Average Structures and Magnetic Properties of $\text{Sr}_2\text{Fe}_{1.5}\text{Cr}_{0.5}\text{O}_5$. *Inorg. Chem.* **2012**, 51 (4), 2638-2644.
21. Ramezanipour, F.; Greedan, J. E.; Cranswick, L. M. D.; Garlea, V. O.; Donaberger, R. L.; Siewenie, J. Systematic Study of Compositional and Synthetic Control of Vacancy and Magnetic Ordering in Oxygen-Deficient Perovskites $\text{Ca}_2\text{Fe}_{2-x}\text{Mn}_x\text{O}_{5+y}$ and $\text{CaSrFe}_{2-x}\text{Mn}_x\text{O}_{5+y}$ ($x = 1/2, 2/3, \text{ and } 1$; $y = 0-1/2$). *J. Am. Chem. Soc.* **2012**, 134 (6), 3215-3227.
22. King, G.; Ramezanipour, F.; Llobet, A.; Greedan, J. E. Local structures of $\text{Sr}_2\text{FeMnO}_{5+y}$ ($y=0, 0.5$) and $\text{Sr}_2\text{Fe}_{1.5}\text{Cr}_{0.5}\text{O}_5$ from reverse Monte Carlo modeling of pair distribution function data and implications for magnetic order. *J. Solid State Chem.* **2013**, 198, 407-415.
23. NIST Center for Neutron Research. <https://www.ncnr.nist.gov/resources/n-lengths/>
24. Farrow, C. L.; Juhas, P.; Liu, J. W.; Bryndin, D.; Božin, E. S.; Bloch, J.; Proffen, T.; Billinge, S. J. L. PDFfit2 and PDFgui: computer programs for studying nanostructure in crystals. *J. Phys.: Condens. Matter* **2007**, 19 (33), 335219.
25. Proffen, T.; Billinge, S. J. L. PDFFIT, a program for full profile structural refinement of the atomic pair distribution function. *J. Appl. Crystallogr.* **1999**, 32 (3), 572-575.
26. Ravel, B.; Newville, M. ATHENA, ARTEMIS, HEPHAESTUS: data analysis for X-ray absorption spectroscopy using IFEFFIT. *Journal of Synchrotron Radiation* **2005**, 12 (4), 537-541.
27. Fuller, C. A.; Berrod, Q.; Frick, B.; Johnson, M. R.; Clark, S. J.; Evans, J. S. O.; Evans, I. R. Brownmillerite-Type $\text{Sr}_2\text{ScGaO}_5$ Oxide Ion Conductor: Local Structure, Phase Transition, and Dynamics. *Chem. Mater.* **2019**, 31 (18), 7395-7404.
28. Stølen, S.; Bakken, E.; Mohn, C. E. Oxygen-deficient perovskites: linking structure, energetics and ion transport. *Phys. Chem. Chem. Phys.* **2006**, 8 (4), 429-447.
29. Fornasini, P.; Beccara, S.; Dalba, G.; Grisenti, R.; Sanson, A.; Vaccari, M.; Rocca, F. Extended x-ray-absorption fine-structure measurements of copper: Local dynamics, anharmonicity, and thermal expansion. *Physical Review B* **2004**, 70 (17), 174301.
30. Takano, M.; Okita, T.; Nakayama, N.; Bando, Y.; Takeda, Y.; Yamamoto, O.; Goodenough, J. B. Dependence of the structure and electronic state of SrFeO_x ($2.5 \leq x \leq 3$) on composition and temperature. *J. Solid State Chem.* **1988**, 73 (1), 140-150.
31. Corallini, S. Structure and dynamics of a new Brownmillerite compound $\text{Sr}_{2-x}\text{Ba}_x\text{ScGaO}_5$ in view of possible application as oxygen ion electrolyte at moderate temperature. Thèse de Doctorat, Université de Rennes 1, 2013.

For Table of Contents Only. Exploring the local structure of the oxygen deficient perovskite $\text{Sr}_2\text{ScGaO}_5$ polymorphs by neutron pair distribution analysis and EXAFS spectroscopy.

